Article

Comparative Purification Strategies for Recombinant Canine Interferon γ in *Escherichia coli*: Denaturing versus Native Conditions

Seungheon Lee [1,2], Donghwan Song [1,2], Sangyoon Kim [3], Jaewon Park [4], HeeJoon Kim [5], and Saerok Shim [1,5,*]

[1] The Institute of YbdY Biotechnology, 83, Gasan Digital 1-ro, Seoul 08589, Republic of Korea
[2] Petstival Animal Hospital, 885 Goyang-daero, Ilsandong-gu, Goyang-si 10319, Republic of Korea
[3] Gangnam 25-si Animal Hospital, 235 Hakdong-ro, Seoul 06053, Republic of Korea
[4] Amazon Animal Hospital, 128 Gyeongchun-ro, Guri-si 11952, Republic of Korea
[5] The Institute of Kulf, Sareung-ro 70 beon-gil, Namyangju-si 12231, Republic of Korea
* Correspondence: kon316@naver.com; Tel.: +82-2-457-0868; Fax: +82-2-2030-7788
Received: 6 November 2025; Revised: 2 December 2025; Accepted: 9 December 2025; Published: 19 December 2025

Abstract: Interferon gamma (IFNγ) is a critical cytokine that activates various immune cells, including macrophages, NK cells, T cells, and even non-immune cells, to fight particularly intracellular infections and cancers. But to use this as medicine for dogs, it is necessary to purify IFNγ for dogs due to its species-specificity. However, efficient purification protocols for recombinant canine IFNγ (rcIFNγ) from *Escherichia coli* that ensure protein stability remain poorly established. In this study, we systematically compared two distinct purification strategies: a denaturing method (lysis with urea) and a native method (lysis without urea), each followed by subsequent purification steps. The two strategies yielded markedly different outcomes. The denaturing protocol resulted in a highly pure and intact monomeric protein. In contrast, the native protocol led to severe proteolytic degradation of the rcIFNγ, resulting in multiple smaller fragments. This present study suggests that it is crucial to explore various conditions for developing stable purification protocols and formulations for rcIFNγ.

Keywords: type II interferon; IFNγ; recombinant protein; canine; protein purification

1. Introduction

Interferons (IFNs), which were discovered in 1957, are structured into three families: Type I, Type II, and Type III (IFN-like cytokines). Although other families have various kinds of subtypes, type 2 IFN consists of only one type, IFNγ [1,2]. The induction of IFNγ is an indirect, multi-step cascade. It begins when Pattern Recognition Receptors (PRRs) on innate immune cells detect Pathogen-Associated Molecular Patterns (PAMPs). This sensing event stimulates these cells to secrete key intermediary cytokines, notably IL-12 and IL-18. These cytokines induce cells such as T cells, natural killer cells, and natural killer T cells to secrete IFNγ. Subsequently, it binds to IFNγ receptor (IFNGR), a tetrameric complex formed from two constitutively expressed IFNGR1 subunits and two conditionally expressed IFNGR2 subunits. This ligand binding initiates the Janus kinase (JAK)-Signal Transducers and Activators of transcription (STAT) signaling pathway. This proximity brings the associated kinases, JAK1 (on IFNGR1) and JAK2 (on IFNGR2), into proximity, allowing them to cross-tyrosine-phosphorylate and activate each other. The activated JAKs then phosphorylate a Tyrosine 440 (Y440) on the intracellular tail of IFNGR1, creating a docking site. This docking site recruits STAT1. Once bound, STAT1 is itself phosphorylated by the JAKs, crucially on Tyrosine 701. This tyrosine-phosphorylated STAT1 then dissociates from the receptor, forms a homodimer, proceeds to the nucleus, and targets to γ-Activated Site (GAS) elements. This binding triggers the genetic transcriptional activation of numerous Interferon-Stimulated Genes (ISGs), including critical anti-pathogen effectors like GBP, IRG, OAS, MX1, and others [3–8].

The human IFNγ gene (IFNG) was isolated in 1982 and is located on chromosome 12 [8,9]; while the canine IFNγ gene is located on chromosome 10 (NCBI Gene ID 403801). IFNγ polypeptides from humans (NP_000610.2) and dogs (NP_001003174.1) are both 166 amino acids (aa) long and share 65.7% sequence identity (calculated using alignment). Both proteins possess a 23 aa signal peptide, but their mature forms differ in length.

The mature human IFNγ is 138 aa, while the mature canine IFNγ is 143 amino acids. Consequently, these mature forms share 63.8% identity (calculated using alignment). This sequence divergence is critical, as the interferon family is known to exhibit species-specificity. For instance, previous studies on Type 1 IFNs demonstrated that porcine IFNα8 showed antiviral activity in bovine (MDBK) cells but was ineffective in human (WISH) and canine (MDCK) cells [10]. Similarly, chicken IFNα3 was active only in avian cells, failing to protect mammalian cells [11]. This species-specificity underscores the necessity of using species-matched canine IFNγ for studies involving canine cells or veterinary applications.

The purification of recombinant human IFNγ (rhIFNγ) is well-established, with numerous studies reporting successful methods from various expression systems, including *Escherichia coli* (*E. coli*) [12,13], Chinese hamster ovary (CHO) cells [14,15], and *Spodoptera frugiperda* (SF9) cells [15]. In contrast, research on the purification of recombinant canine IFNγ (rcIFNγ) is significantly more limited. While the production of rcIFNγ in *E. coli* [16,17] and silkworms (*Bombyx mori*) [16,18] has been reported, systematic studies comparing different strategies or optimizing the purification method for rcIFNγ are still lacking.

Therefore, we aimed to compare two distinct purification strategies for rcIFNγ expressed in *E. coli*: a denaturing condition (Condition A, with 8 M urea) and a native condition (Condition B, without 8 M urea). The goal was to provide a foundational comparison of the biochemical properties (molecular weight, purity, stability, and yield) resulting from each approach. This comparison provides a basis for the future development of purification protocols intended for functional studies.

2. Material and Methods

2.1. Expression of Recombinant Proteins Using E. coli

Expression vector (pPROExHTa) containing mature cIFNγ (without 23aa signal peptide at the *N*-terminus, Figure S1) was transformed into *E. coli* (BL21/Codon plus). The bacteria grew at 37 °C until the cell density, measured as an optical density (OD) value at 600 nm, reached a value of 0.6 OD. 0.6 mM isopropyl β-D-1-thiogalactopyranoside (IPTG; Cellconic, Hanam, Republic of Korea) was added to the cultured broth for 4 h at 37 °C to induce target protein expression. After induction, the cells were centrifuged for 20 min at 6000 rpm at 4 °C, and all supernatants were decanted, leaving the *E. coli* pellet.

2.2. Initial Capture of rcIFNγ via Affinity Chromatography

The *E. coli* pellets were resuspended in equal volumes of two different 50 mM sodium phosphate (Bio Basic Inc., Markham, ON, Canada), 0.3 M Sodium chloride (Cellconic), pH 7.0 buffers: one containing 8 M urea (Condition A) and the other without 8 M urea (Condition B). The supernatant containing His^6-tag proteins was then loaded onto TALON® Magnetic Beads (Takara, Kusatsu, Japan). After measuring their concentration using the NanoDrop spectrophotometer (Thermo Fisher Scientific Inc., Waltham, MA, USA) and Bradford assay, the samples were loaded into SDS-PAGE gels. These were stained with Coomassie Brilliant Blue solution to check the size and pattern of the purified recombinant proteins.

2.3. Polishing of rcIFNγ Using Other Chromatography

The confirmed elution fractions under both conditions were tested to ensure their stability without any additives by dialysis. Based on the stability results, thereafter, the fractions, which remained soluble without additives, were purified through Anion Exchange Chromatography (AEC) utilizing a HisTrap Q FF™ column (GE Healthcare, Chicago, IL, USA). Conversely, the unstable (aggregated) fractions were purified by a High-Performance Liquid Chromatography (HPLC) column from Grace (Stockbridge, GA, USA). Since the purified rcIFNγ showed poor solubility (Condition A), sodium dodecyl sulfate (SDS; Biosesang, Yongin, Republic of Korea) was added to the fractions at 0.1% (*w*/*v*) to ensure solubilization. The purified proteins were then analyzed by silver staining with Bovine Serum Albumin (BSA) and Bicinchoninic acid (BCA) assay to determine their pattern and concentration.

3. Results

3.1. Comparison after the Initial Capture Step

The cIFNγ gene in the pPROExHTa vector was expressed in the *E. coli* BL21/Codon plus. After lysis of the *E. coli* pellet under Condition A (with 8 M urea) or Condition B (without urea), these supernatants were loaded into a mini-TALON affinity column. The elution samples from the Talon affinity column were visualized by

Coomassie brilliant blue staining. The expected molecular weight of the recombinant protein was approximately 20.58 kDa, as predicted by the Compute pI/Mw program (https://web.expasy.org/compute_pi/ accessed on 6 April 2025). The dominant bands from Condition A corresponded to the expected size (Figure 1A). However, the major bands from Condition B seemed to be slightly higher than the expected size (Figure 1B). When tested for stability without additives using a dialysis method, the recombinant protein purified under Condition A tended to be aggregated, whereas that purified under Condition B remained soluble. Based on these results, we performed HPLC (Figure 2) using Condition A samples and AEC with Condition B samples (Figure 3).

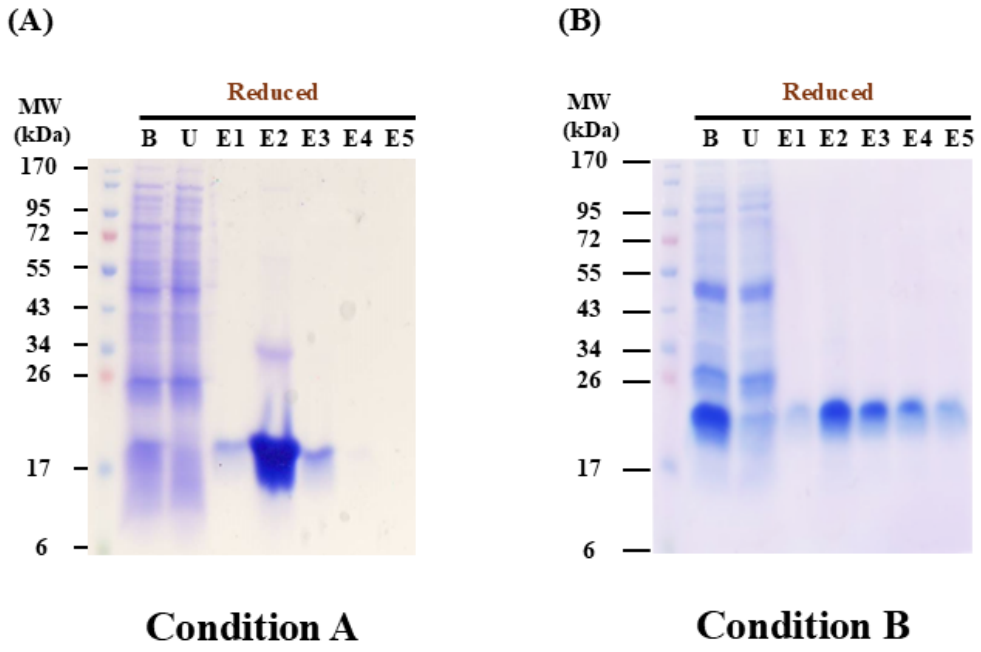

Figure 1. The purification of recombinant canine Interferon gamma (rcIFNγ) with pPROExHTa from *Escherichia coli* with Talon affinity chromatography. Elution fractions (E1–E5) of rcIFNγ were resolved by SDS-PAGE. An equal volume of each fraction was loaded, corresponding to 10 μg of protein for the peak fraction (E2) as quantified by Nanodrop. The gel was visualized by Coomassie brilliant blue staining. (**A**) Purification under Condition A (with 8 M Urea). A prominent band was observed at approximately 21 kDa, which corresponds to the predicted size of rcIFNγ (20.58 kDa). (**B**) Purification under Condition B (without 8 M Urea). A prominent band was observed at approximately 23 kDa, which is slightly larger than the predicted size. kDa, kilodalton; Reduced, each sample was boiled with dithiothreitol (DTT); B, initial sample before loading onto the column; U, unbound fraction that flowed through the column.

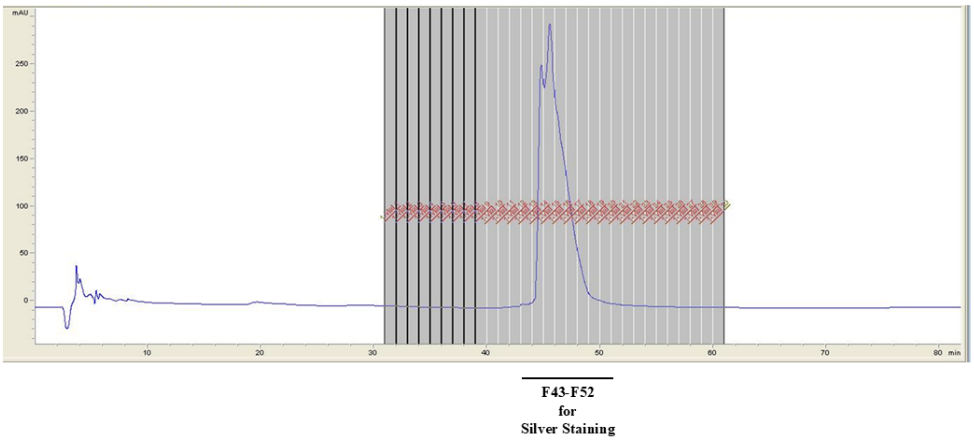

Figure 2. The purification of recombinant canine Interferon gamma (rcIFNγ) (condition A) by High-Performance Liquid Chromatography (HPLC). UV absorbance at 280 nm (blue line) was recorded during the polishing step with HPLC. The Y axis shows UV absorbance (mAU) and the X axis shows retention time (min). The horizontal black line indicates the elution fractions number from 43 to 52.

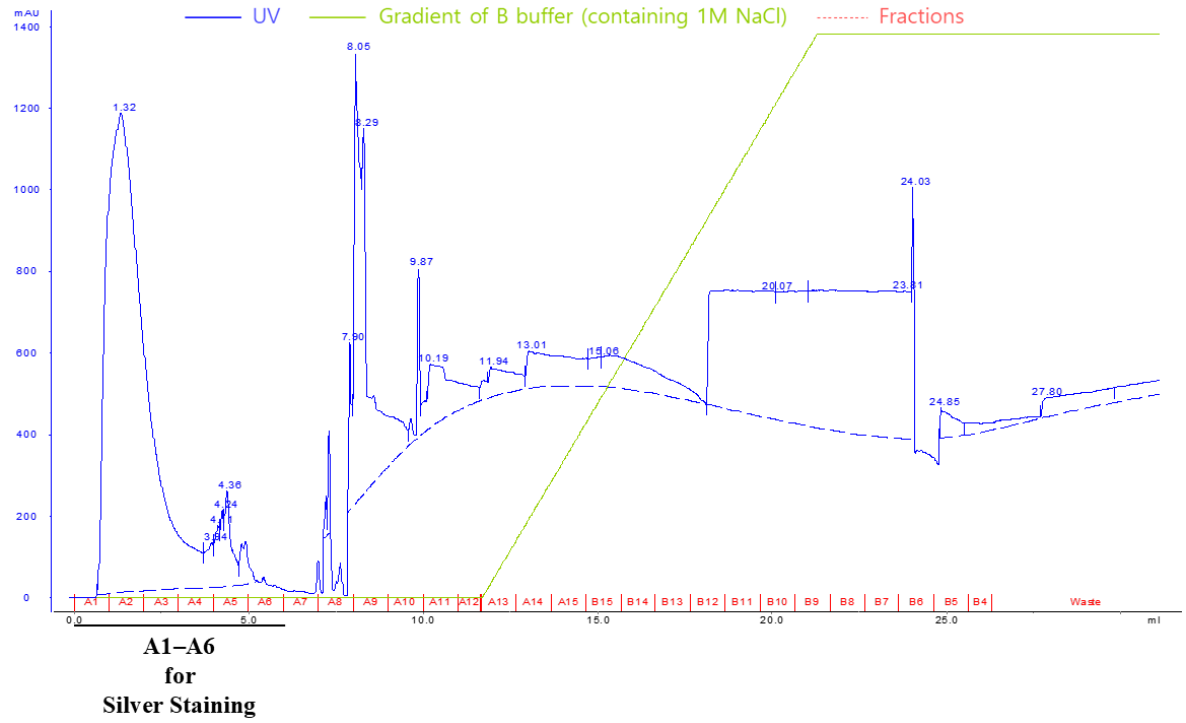

Figure 3. The purification of recombinant canine Interferon gamma (rcIFNγ) (condition B) by anion exchange chromatography. UV absorbance at 280 nm was recorded during the polishing step. The Y axis shows UV absorbance (mAU) and the X axis shows retention volume (ml). The horizontal black line indicates the elution fractions (A1–A6).

3.2. Comparison after the Polishing Step

After the polishing step, the protein obtained under Condition B remained soluble in the native buffer; however, the protein from Condition A did not. Therefore, 0.1% SDS was added to the Condition A sample, and both samples were visualized by silver staining. In Condition A, the purity increased, as indicated by the disappearance of non-target bands (Figure 4A), whereas in Condition B, the purity did not improve compared to the initial capture step (Figure 5), likely due to degradation. For Condition A sample whose bands were shown as one band, silver staining with known concentrations of bovine serum albumin (BSA) was performed to measure the concentration of rcIFNγ (Figure 4B). In contrast, this analysis was not performed for Condition B sample, given its low purity and the presence of multiple degradation bands (Figure 5).

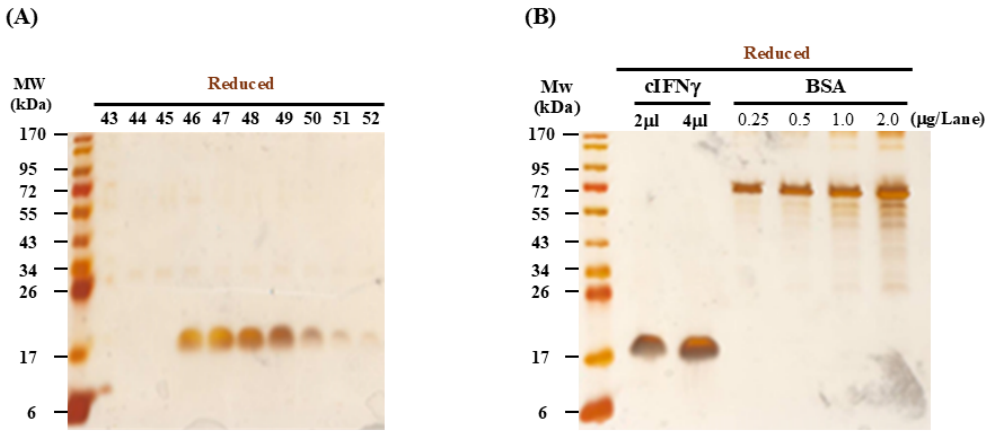

Figure 4. The silver staining result of recombinant canine Interferon gamma (rcIFNγ) (condition A) purified by High-Performance Liquid Chromatography (HPLC). (**A**) An equal volume of each fraction corresponding to the UV peak in Figure 2 was loaded. (**B**) The band intensity of rcIFNγ (condition A) was compared to the intensities of known concentrations of bovine serum albumin. kDa, kilodalton; Reduced, each sample was boiled with dithiothreitol (DTT).

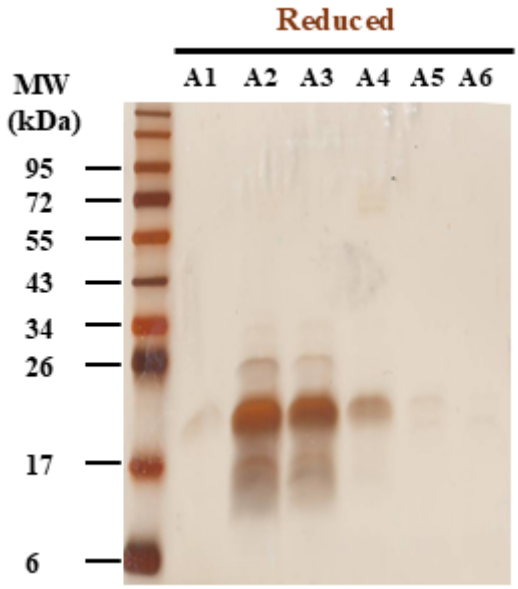

Figure 5. The silver staining result of recombinant canine Interferon gamma (rcIFNγ) (condition B) purified by anion exchange chromatography. An equal volume of each fraction corresponding to the UV peak in Figure 3 was loaded. kDa, kilodalton; Reduced, each sample was boiled with dithiothreitol (DTT).

4. Discussion

The trend of human-animal cohabitation is increasing, with many people viewing companion animals, such as dogs and cats, as partners. Consequently, the demand for effective and species-specific veterinary therapeutics is also on the rise [19,20]. Among the critical immunomodulators, IFNs play a pivotal role. For instance, recombinant feline IFNω is widely used in veterinary practice [21]. However, the IFN family is known for its high species-specificity [10,11,22], underscoring the necessity of developing canine-specific IFN therapeutics rather than relying on cross-species applications. Although the production of rcIFNγ in *E. coli* has been reported [16,17], systematic comparison studies to explore appropriate purification strategies remain lacking.

In this study, we compared two purification strategies for rcIFNγ expressed in *E. coli*. Following the initial capture step using TALON affinity chromatography, dominant bands matching the theoretical molecular weight of rcIFNγ (approx. 20.6 kDa) were observed under both conditions (Figure 1). However, two critical differences were immediately apparent. First, an additional band at approximately 34 kDa, which is likely an artificial, non-native dimer, was shown under Condition A (with 8 M Urea) (Figure 1A). Second, although E2 (the peak elution fraction) from both conditions was loaded at an equal amount (10 μg) as quantified by NanoDrop, the rcIFNγ band from Condition A appeared significantly thicker than the band from Condition B. This observation strongly correlated with a quantification discrepancy noted between the Nanodrop and Bradford assays. For Condition A, the protein concentration measured by the Bradford assay was consistently higher than the value from the Nanodrop. In contrast, for Condition B, this pattern was reversed (NanoDrop > Bradford). This discrepancy suggests a fundamental difference in the protein's folding state, as the Nanodrop relies on the absorbance of aromatic amino acids (Tryptophan and Tyrosine) at 280 nm [23], whereas the Bradford assay (Coomassie dye) binds primarily to basic residues (e.g., Arginine, Lysine) [24].

After the initial capture step, when additives (like urea and sodium chloride) were removed during a dialysis test, almost all the protein from Condition A (urea-purified) was heavily aggregated. In contrast, the protein from Condition B (native-purified) remained fully soluble. This result is scientifically logical: the rcIFNγ from condition A, which was kept artificially unfolded by 8 M Urea, failed to refold correctly upon removal of the denaturant and aggregated [25]. Conversely, Condition B protein was already in its stable, native conformation. This difference in stability was the decisive factor for the subsequent purification steps. The stable, native protein from Condition B was compatible with a native-state method (AEC) (Figure 3). However, the unstable protein from Condition A was clearly incompatible with native buffers and thus required a denaturing-compatible method (HPLC) (Figure 2). Consistent with this instability, the protein from Condition A still required the addition of 0.1% SDS post-HPLC to maintain solubility for the final analysis.

The silver stain analysis of the final, 2nd-purification products revealed a stark divergence in purity. For Condition A (Figure 4), the HPLC step was highly effective, yielding a single, dominant band corresponding to

the rcIFNγ monomer, which was a clear improvement from the initial purification (Figure 1A). In contrast, the purity of Condition B (Figure 5) did not improve after the AEC step. While Figure 4 showed the rcIFNγ primarily as a single band, Figure 5 showed multiple smaller fragments, including a dominant band (at least four distinct bands). This degradation in Condition B is likely attributable to residual *E. coli* proteases that remained active despite the several washing steps [26]. In Condition A, these trace proteases were effectively rendered inactive by the strong denaturing effects of both the 8 M urea and the organic solvents (acetonitrile) used during HPLC. Conversely, the native buffers used in Condition B allowed these proteases to remain active, leading to the proteolytic degradation of the rcIFNγ. This vulnerability exists because the rcIFNγ, being expressed in *E. coli*, is non-glycosylated and therefore lacks the protective carbohydrates that shield its native, mammalian-expressed counterpart from proteolytic attack [27]. Nevertheless, the *E. coli* expression system remains a preferred choice, due to its advantages in cost-effectiveness, rapid production, and high yield potential compared to mammalian systems [28,29]. Despite this dramatic difference in final purity (High Purity A vs. Degraded B), the final quantification—combining data from the BCA assay and silver staining with BSA (Figure 4B)—showed that the approximate total protein yield was similar for both conditions across several replications.

In summary, we compared two distinct purification strategies for rcIFNγ expressed in *E. coli*: Condition A (with 8 M Urea) and Condition B (without 8 M Urea). While the final yield of protein—a key factor in productivity—was found to be similar for both conditions, there were differences in the biochemical properties: (1) the folding state, (2) stability in native buffers, and (3) final purity. These differences suggest the importance of selecting an appropriate purification strategy, as this choice directly impacts the protein's final state and subsequent pharmaceutical formulation [30]. Regrettably, the biological activities of the two purified rcIFNγ were not assessed in this study. Therefore, future in vitro studies using canine cell lines, such as MDCK or primary cells, are necessary to compare their activities. This work can lay a foundation for the future development of species-specific canine medicines.

Supplementary Materials: The following supporting information can be downloaded at: https://media.sciltp.com/articles/others/2512101611044690/JIIM-25110031-Author-supplementary-figure-V2.pdf. Figure S1: Amino acid sequences of native and recombinant canine IFN gamma (cIFNγ).

Author Contributions: S.L.: conceptualization, methodology, formal analysis, investigation; D.S.: investigation; S.K., J.P.: data curation, formal analysis; H.K.: conceptualization; S.S.: conceptualization, supervision, writing—reviewing and editing. All authors have read and agreed to the published version of the manuscript.

Funding: This research received no external funding

Institutional Review Board Statement: Not applicable.

Informed Consent Statement: Not applicable.

Data Availability Statement: Not applicable.

Conflicts of Interest: The authors declare no conflict of interest.

Use of AI and AI-Assisted Technologies: No AI tools were utilized for this paper.

Abbreviations

aa, amino acids; AEC, Anion Exchange Chromatography; BCA, Bicinchoninic acid; BSA, Bovine Serum Albumin; CHO, Chinese hamster ovary; *E. coli*, *Escherichia coli*; GAS, γ-Activated Site; HPLC, High-Performance Liquid Chromatography; IFNs, Interferons; IPTG, isopropyl β-D-1-thiogalactopyranoside; ISGs, Interferon-Stimulated Genes; JAK, Janus kinase; OD, optical density; PAMPs, Pathogen-Associated Molecular Patterns; PRRs, Pattern Recognition Receptors; rcIFNγ, recombinant canine IFNγ; rhIFNγ, recombinant human IFNγ; SDS, sodium dodecyl sulfate; STAT, Signal Transducers and Activators of transcription.

References

1. Isaacs, A.; Lindenmann, J. Virus Interference: I. The Interferon. *CA A Cancer J. Clin.* **1988**, *38*, 280–290. https://doi.org/10.3322/canjclin.38.5.280.
2. Pestka, S. The interferons: 50 years after their discovery, there is much more to learn. *J. Biol. Chem.* **2007**, *282*, 20047–20051. https://doi.org/10.1074/jbc.R700004200.
3. Borden, E.C.; Sen, G.C.; Uze, G.; Silverman, R.H.; Ransohoff, R.M.; Foster, G.R.; Stark, G.R. Interferons at age 50: Past, current and future impact on biomedicine. *Nat. Rev. Drug Discov.* **2007**, *6*, 975–990. https://doi.org/10.1038/nrd2422.
4. Walker, F.C.; Sridhar, P.R.; Baldridge, M.T. Differential roles of interferons in innate responses to mucosal viral infections. *Trends Immunol.* **2021**, *42*, 1009–1023. https://doi.org/10.1016/j.it.2021.09.003.

5. Sekimoto, T.; Nakajima, K.; Tachibana, T.; Hirano, T.; Yoneda, Y. Interferon-gamma-dependent nuclear import of Stat1 is mediated by the GTPase activity of Ran/TC4. *J. Biol. Chem.* **1996**, *271*, 31017–31020. https://doi.org/10.1074/jbc.271.49.31017.
6. Quelle, F.W.; Thierfelder, W.; Witthuhn, B.A.; Tang, B.; Cohen, S.; Ihle, J.N. Phosphorylation and activation of the DNA binding activity of purified Stat1 by the Janus protein-tyrosine kinases and the epidermal growth factor receptor. *J. Biol. Chem.* **1995**, *270*, 20775–20780. https://doi.org/10.1074/jbc.270.35.20775.
7. Alspach, E.; Lussier, D.M.; Schreiber, R.D. Interferon gamma and Its Important Roles in Promoting and Inhibiting Spontaneous and Therapeutic Cancer Immunity. *Cold Spring Harb. Perspect. Biol.* **2019**, *11*, a028480. https://doi.org/10.1101/cshperspect.a028480.
8. Mertowska, P.; Smolak, K.; Mertowski, S.; Grywalska, E. Immunomodulatory Role of Interferons in Viral and Bacterial Infections. *Int. J. Mol. Sci.* **2023**, *24*, 10115. https://doi.org/10.3390/ijms241210115.
9. Gray, P.W.; Goeddel, D.V. Structure of the human immune interferon gene. *Nature* **1982**, *298*, 859–863. https://doi.org/10.1038/298859a0.
10. Kim, E.; Jhun, H.; Kim, J.; Park, U.; Jo, S.; Kwak, A.; Kim, S.; Nguyen, T.T.; Kang, Y.; Choi, I.; et al. Species Specific Antiviral Activity of Porcine Interferon-alpha8 (IFNalpha8). *Immune Netw.* **2017**, *17*, 424–436. https://doi.org/10.4110/in.2017.17.6.424.
11. Yoon, M.; Lee, S.; Song, D.; Hwang, J.; Kim, H.; Yoo, H.; Choi, M.; Kim, S. Antiviral Activity of Gallus Recombinant Interferon α3. *J. Inflamm. Infect. Med.* **2025**, *1*, 2504000509. https://doi.org/10.53941/jiim.2025.100006.
12. Petrov, S.; Nacheva, G.; Ivanov, I. Purification and refolding of recombinant human interferon-gamma in urea-ammonium chloride solution. *Protein Expr. Purif.* **2010**, *73*, 70–73. https://doi.org/10.1016/j.pep.2010.03.026.
13. Zhu, F.; Wang, Q.; Pu, H.; Gu, S.; Luo, L.; Yin, Z. Optimization of soluble human interferon-gamma production in *Escherichia coli* using SUMO fusion partner. *World J. Microbiol. Biotechnol.* **2013**, *29*, 319–325. https://doi.org/10.1007/s11274-012-1185-0.
14. Devos, R.; Opsomer, C.; Scahill, S.J.; Van der Heyden, J.; Fiers, W. Purification of recombinant glycosylated human gamma interferon expressed in transformed Chinese hamster ovary cells. *J. Interferon Res.* **1984**, *4*, 461–468. https://doi.org/10.1089/jir.1984.4.461.
15. Zhang, J.; Alfonso, P.; Thotakura, N.R.; Su, J.; Buergin, M.; Parmelee, D.; Collins, A.W.; Oelkuct, M.; Gaffney, S.; Gentz, S.; et al. Expression, purification, and bioassay of human stanniocalcin from baculovirus-infected insect cells and recombinant CHO cells. *Protein Expr. Purif.* **1998**, *12*, 390–398. https://doi.org/10.1006/prep.1997.0857.
16. Uchino, T.; Yamada, K.; Okano, F.; Satoh, M.; Kawakami, I. Use of Canine Interferon-Γ (Ifn-Γ) το Treat Non-Atopic Dermatitis. U.S. Patent No. 5,955,069, 21 September 1999.
17. Zucker, K.; Lu, P.; Asthana, D.; Carreno, M.; Yang, W.C.; Esquenazi, V.; Fuller, L.; Miller, J. Production and characterization of recombinant canine interferon-gamma from *Escherichia coli*. *J. Interferon Res.* **1993**, *13*, 91–97. https://doi.org/10.1089/jir.1993.13.91.
18. Okano, F.; Satoh, M.; Ido, T.; Okamoto, N.; Yamada, K. Production of canine IFN-gamma in silkworm by recombinant baculovirus and characterization of the product. *J. Interferon Cytokine Res.* **2000**, *20*, 1015–1022. https://doi.org/10.1089/10799900050198462.
19. Brown, A. About half of U.S. Pet Owners Say Their Pets Are as Much a Part of Their Family as a Human Member. Available online: https://www.pewresearch.org/short-reads/2023/07/07/about-half-us-of-pet-owners-say-their-pets-are-as-much-a-part-of-their-family-as-a-human-member/?gad_source=1&gad_campaignid=22378837192&gbraid=0AAAAA-ddO9Ev9IRHLygOXRt20zIWNMeTw&gclid=Cj0KCQjwgpzIBhCOARIsABZm7vEmaQvgchLhUboqRgiB7ld0nkW7S7JKRhkEhyKYGhghQ346FGtu538aAhGwEALw_wcB (accessed on 3 November 2025).
20. Grand View Research. *Veterinary Medicine Market Size, Share & Trends Analysis Report by Product (Biologics, Pharmaceuticals), by Animal Type, by Route of Administration, by Distribution Channel, by Region, and Segment Forecasts*; Grand View Research: San Francisco, CA, USA, 2024.
21. Li, S.F.; Zhao, F.R.; Shao, J.J.; Xie, Y.L.; Chang, H.Y.; Zhang, Y.G. Interferon-omega: Current status in clinical applications. *Int. Immunopharmacol.* **2017**, *52*, 253–260. https://doi.org/10.1016/j.intimp.2017.08.028.
22. Samuel, C.E.; Farris, D.A. Mechanism of interferon action. Species specificity of interferon and of the interferon-mediated inhibitor of translation from mouse, monkey, and human cells. *Virology* **1977**, *77*, 556–565. https://doi.org/10.1016/0042-6822(77)90481-0.
23. Warburg, O.; Christian, W. Isolierung und Kristallisation des Grungsferments Enolase. *Die Naturwissenschaften* **1941**, *29*, 589–590. https://doi.org/10.1007/bf01482279.
24. Bradford, M.M. A rapid and sensitive method for the quantitation of microgram quantities of protein utilizing the principle of protein-dye binding. *Anal. Biochem.* **1976**, *72*, 248–254. https://doi.org/10.1016/0003-2697(76)90527-3.
25. Gupta, V.; Sengupta, M.; Prakash, J.; Tripathy, B.C. Production of Recombinant Pharmaceutical Proteins. In *Basic and Applied Aspects of Biotechnology*; Gupta, V., Sengupta, M., Prakash, J., Tripathy, B.C., Eds.; Springer: Singapore, 2017; pp. 77–101.

26. Ryan, B.J.; Henehan, G.T. Overview of approaches to preventing and avoiding proteolysis during expression and purification of proteins. *Curr. Protoc. Protein Sci.* **2013**, *71*, 5–25. https://doi.org/10.1002/0471140864.ps0525s71.
27. Sareneva, T.; Pirhonen, J.; Cantell, K.; Julkunen, I. N-glycosylation of human interferon-gamma: Glycans at Asn-25 are critical for protease resistance. *Biochem. J.* **1995**, *308*, 9–14. https://doi.org/10.1042/bj3080009.
28. Schutz, A.; Bernhard, F.; Berrow, N.; Buyel, J.F.; Ferreira-da-Silva, F.; Haustraete, J.; van den Heuvel, J.; Hoffmann, J.E.; de Marco, A.; Peleg, Y.; et al. A concise guide to choosing suitable gene expression systems for recombinant protein production. *STAR Protoc.* **2023**, *4*, 102572. https://doi.org/10.1016/j.xpro.2023.102572.
29. Jaffe, S.R.; Strutton, B.; Levarski, Z.; Pandhal, J.; Wright, P.C. *Escherichia coli* as a glycoprotein production host: Recent developments and challenges. *Curr. Opin. Biotechnol.* **2014**, *30*, 205–210. https://doi.org/10.1016/j.copbio.2014.07.006.
30. Ribeiro, R.; Abreu, T.R.; Silva, A.C.; Gonçalves, J.; Moreira, J.N. Insights on the Formulation of Recombinant Proteins. In *Current Applications of Pharmaceutical Biotechnology*; Silva, A.C., Moreira, J.N., Lobo, J.M.S., Almeida, H., Eds.; Springer International Publishing: Cham, Switzerland, 2020; pp. 23–54.